Molecular Dynamics and Experimental Investigations of Membrane Perturbation by Ceragenin CSA-13

R. Jueati[1], J. Jittikoon[2], O. Vajragupta[1], and J. Pimthon[1]*

[1] *Department of Pharmaceutical Chemistry, Faculty of Pharmacy, Mahidol University, Bangkok, Thailand*
[2] *Department of Biochemistry, Faculty of Pharmacy, Mahidol University, Bangkok, Thailand*

Abstract

Ceragenin CSA-13, a cholic acid derivative, has been reported as a novel template/scaffold for development of more potent and specific antibiotics. However, the exact mechanism of ceragenin CSA-13 action is not completely understood. This study aimed at investigating the molecular mechanism of membrane disruption by ceragenin CSA-13 using molecular dynamics (MD) simulations and experimental studies. Our findings showed that CSA-13 effectively induces calcein leakage when interacted with negatively charged DOPG vesicles, while exhibited weak dye-leakage activity for DOPC vesicles. The experimental results are very well in agreement with the MD calculations, where we observed the insertion of ceragenin CSA-13 molecules into PG bilayer membrane, induced an increase membrane fluidity and resulting in the membrane destabilization.

KEYWORDS: MD Simulation, cholic acid-derived antimicrobial agents, calcein leakage, lipid membranes, interaction

INTRODUCTION

The increased occurrence of antibiotic-resistant bacterial strains has led to the need for exploring new agents with novel mechanisms of action that can circumvent established target site-based resistance. In recent years, several series of cholic acid-derived compounds have attracted considerable attention because of their effectiveness against a wide range of microorganisms including several antibiotic-resistant strains[1-3]. Moreover, they show a high degree of selectivity for killing microbe compared to host mammalian cells[4].

Ceragenin CSA-13, a synthetic derivative of cholic acid with a pendant aminoalkyl group, was developed by Savage et al (Figure 1) (3). This compound shows significant ability to kill bacteria including multidrug-resistant pathogens at very low concentration and exhibits low toxicity, which demonstrate potential as novel therapeutic agents[5]. Unfortunately, the precise mechanism of action is not entirely clear. It has been speculated that ceragenin CSA-13 interacts with lipid components of the bacterial cell membrane leading to depolarization of the membrane and, further, to cell death[6]. It is therefore crucial to understand the mechanism of membrane permeation in order to develop ceragenin CSA-13 and its analogues as future antibiotics.

The membranes surrounding cellular organelles have different and characteristic lipid compositions. In general, the outer leaflet of the mammalian cell membrane is comprised mainly of zwitterionic phosphatidylcholine (PC) and phosphatidylethanolamine (PE). In contrast, bacterial membranes are rich in negatively charged phospholipids, such as phosphatidylglycerol (PG)[6]. The subtle differences in the lipid composition in various mammalian cell membranes may contribute to differ in their susceptibilities to ceragenin CSA-13.

*Corresponding author: Department of Pharmaceutical Chemistry, Faculty of Pharmacy, Mahidol University. 447 Sri Ayudthaya Road, Rajthevi, Bangkok, 10400, Thailand. Tel.: +66 2 6448677 ext. 5407; fax: +66 26448695 E-mail address: jutarat.pim@mahidol.ac.th
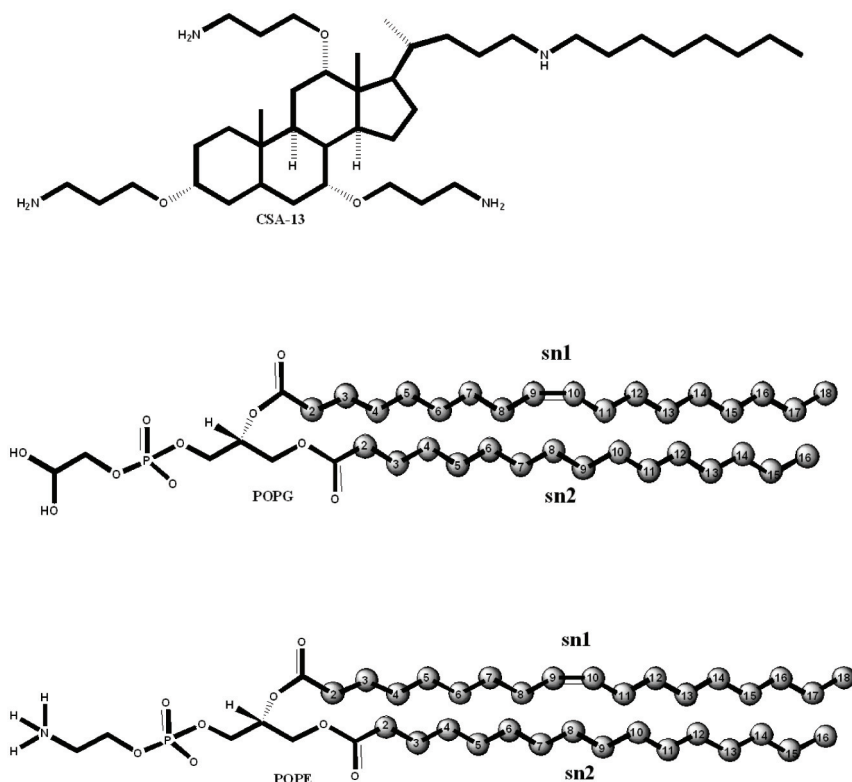
Figure 1. Chemical structures of ceragenin CSA-13, POPG, POPE

This study aims to complement MD simulations and experimental studies for investigate interaction between ceragenin CSA-13 and model membranes of different lipid types to better understand the mode of action of ceragenins. By means of MD simulation, the palmitoyloleoylphosphatidylglycerol (POPG) bilayer was used to mimic a bacterial cell membrane, while the palmitoyloleoyl-phosphatidylethanolamine (POPE) bilayer was used to mimic a human cell membrane. In experimental studies, membrane perturbation effects of the ceragenin CSA-13 were investigated through the leakage of calcein from large unilamellar vesicles (LUVs) of various lipid compositions.

MATERIALS AND METHODS

Molecular dynamics simulations: All simulations and analyses were performed with the CHARMM package[7] using the all atom CHARMM36 force field for lipids[8], CHARMM General Force Field (CGenFF) for drug-like molecules[9] and the modified TIP3P water model.[10] The leapfrog Verlet algorithm was applied in all simulations with a time step of 2 fs. Simulations were run in tetragonal periodic boundary conditions in the constant number of atoms (N), constant normal pressure (P = 1 atm), constant surface tension (γ = 0 mN/m), and a constant temperature (T = 303 K) or NPγT ensemble. All hydrogen atoms were constrained using the SHAKE algorithm.

The structure of ceragenin CSA-13 was constructed using Material studio 5.0 (Accelrys, USA). The starting coordinates of a monocomponent phospholipid bilayer were obtained from a 150 ns pre-equilibrated patch of 224 lipids (manuscript in preparation) and cut to generate a 144-lipid system. The phospholipid was either POPG or POPE. A solvated phospholipid bilayer was equilibrated

for 10 ns and the area per lipid and lamellar spacing were monitored. For the characterization of ceragenin CSA-13/membrane interactions, the model systems contained (i) 3 ceragenin CSA-13, 144 POPG lipids, 10685 water molecules, 162 sodium ions, and 30 chloride ions (Figure 2a and 2b) (ii) 3 ceragenin CSA-13, 144 POPE lipids, 10160 water

molecules, 17 sodium ions, and 28 chloride ions (Figure 2d and 2e). 6-ns MD simulations were performed on both systems. Notice that the interaction effects were explored at high concentration of ceragenin CSA-13. These simulations were run using the same simulation procedure as described by Pimthon et al.[11]
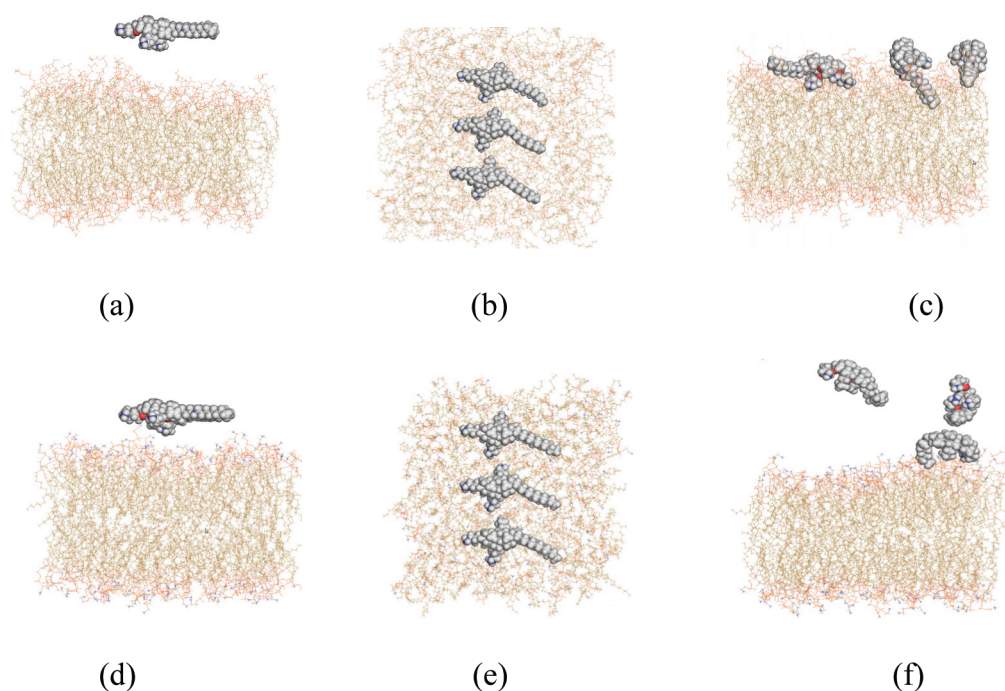

(a)   (b)   (c)

(d)   (e)   (f)

Figure 2. Simulation model. (a) Side view and (b) top view of the initial configuration of ceragenin CSA-13/POPG, (c) side view of the ceragenin CSA-13/POPG at 6 ns, (d) side view and (e) top view of the initial configuration of ceragenin CSA-13/POPE, (f) side view of the ceragenin CSA-13/POPE at 6 ns. The ceragenin CSA-13 is shown as sphere. The lipid bilayer is shown as line. Water and counterions have been omitted for visual clarity.

Model of ceragenin CSA-13 induced calcein leakage from liposomes:

Materials: Dioleoylphosphatidylglycerol (DOPG), dioleoylphosphatidylcholine (DOPC), and dioleoylphosphatidylethanolamine (DOPE) of purity 99%, were purchased from Avanti Polar Lipids (Alabaster, AL) and used without further purification. The ceragenin CSA-13 was a gift from Professor Paul Savage (Brigham Young University, USA).

Vesicle preparation: LUVs were prepared and characterized as described by Sroda et al.[12] Briefly, DOPG, DOPC, and DOPG/DOPE

(at a mol ratio of 7:3 and 3:7) were dissolved in chloroform. Lipids were dried under a stream of nitrogen and then under vacuum overnight to completely remove any residual solvent. The thin lipid film was then dispersed in Hepes buffer (10 mM Hepes, 150 mM NaCl, 1 mM EDTA, pH = 7.4) to a concentration of 5 μM. For the leakage experiments, the lipid was hydrated with a buffer containing 70 mM calcein. The liposome suspension was extruded for 50 times at room temperature through neucleophore polycarbonate membranes with 400 nm pores. The untrapped calcein was removed by passing the liposome suspension

through a sephadex G-50 gel filtration column. Leakage of calcein from liposomes was monitored after 5 min incubation with ceragenin CSA-13 by measuring fluorescence intensity on a SpectraMax GeminiEm spectrofluorometer (Molecular Devices, CA, USA) at an excitation wavelength of 490 nm and an emission wavelength of 520 nm. For determination of 100 % leakage, Triton X-100 (1 % in Hepes buffer) was added to dissolve the vesicles. The apparent percent leakage value, caused by ceragenin CSA-13, was calculated according to

% apparent leakage = *100 x (F-Fo)/(Ft-Fo)*; where *F* is the fluorescence intensity induced by ceragenin CSA-13, *Ft* denotes the fluorescence intensity corresponding to 100% leakage after the addition of 1% of Triton X-100, and *Fo* represents the fluorescence intensity of intact vesicles.

RESULTS AND DISCUSSIONS

Simulation results: We conducted preliminary MD simulations of the interaction between ceragenin CSA-13 and model lipid membranes. The ceragenin CSA-13 was initially placed in water phase, closed to the membrane/ waterinterface. To determine the locations of ceragenin CSA-13 during a simulated period, we calculated electron density profiles of ceragenin CSA-13 molecules by placing the appropriate number of electrons at the sites of the atomic nuclei, and then binning over the entire configuration space along the membrane normal (z-axis) as shown in Figure 3. From electron density profile, the phosphate groups of lipids were also studied to monitor the depth of insertion of ceragenin CSA-13 molecules in the lipid bilayer. The peaks due to the ceragenin CSA-13 molecules in the ceragenin CSA-13/ POPG model (Figure 3A) overlaps with that of the phosphate atoms, whereas the ceragenin CSA-13 molecules in the ceragenin CSA-13/ POPE model (Figure 3B) is only located near the peak of phosphate moiety of POPE. These confirm the ceragenin CSA-13 spontaneously inserts into the POPG bilayer (Figure 2c), while it either slightly interacts with or

detaches from the POPE membrane (Figure 2f). After adsorption of the ceragenin CSA-13 to the membrane surface, in particular, the change in lipid membrane morphology was monitored by calculating carbon-deuterium order parameters (S_{CD}) for an individual segment of the acyl chain. Experimentally, this parameter can be directly measured by deuterated NMR. In MD simulations, it was calculated as

$$S_{CDi} = \frac{1}{2}\left(3\cos^2\theta_i - 1\right)$$

where θ_i is the (time dependent) angle between the $C_i - H$ bond vector and a reference axis (z-axis). The angular brackets denote a time and ensemble average. The S_{CD} typically ranges from 0 to 0.5. This value gets close to 0 for a chain undergoing isotropic rotation, while it gets close to 0.5, representing a rigidity of hydrophobic chain of phospholipid. The differences of the S_{CD} profile on the two different types of bilayers containing ceragenin CSA-13 is shown in Figure 4A and 4B. In the ceragenin CSA-13/ POPG model (Figure 4A), we found a substantial decrease in deuterium order parameters of the lipid chain for the lipids that are in the ceragenin CSA-13-bound monolayer. On the other hand, there are no pronounced effects on the ceragenin CSA-13-free monolayer and ceragenin CSA-13-bound monolayer in the ceragenin CSA-13/POPE system (Figure 4B). This confirms the selectivity and strong binding of the ceragenin CSA-13 to the negatively charged bacterial membrane over the mammalian cell membrane. Moreover, a decrease in S_{CD} indicated that ceragenin CSA-13 causes increasing mobility of hydrophobic chains of POPG lipids, in turn, the membrane integrity is disturbed.

The deuterium order parameters are plotted for sn1 of lipids in the ceragenin CSA-13-free monolayer (open triangles), and in the monolayer in which the ceragenin CSA-13 bind (open circles); sn2 of lipids in the ceragenin CSA-13-free monolayer (solid triangles), and in the monolayer, in which the ceragenin CSA-13 bind (solid circles).
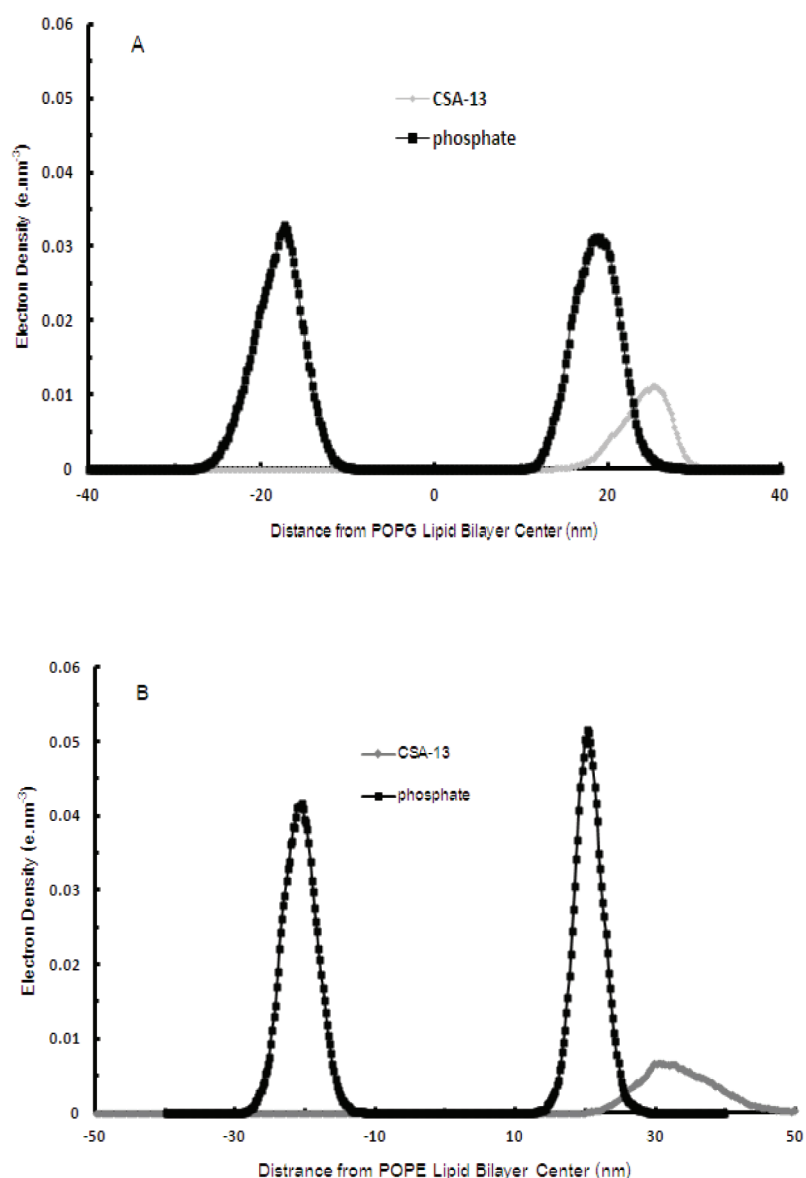
Figure 3. The electron density profiles for ceragenin CSA-13 and for the phosphate group of (A) POPG and (B) POPE bilayer.

Experimental results: For the current preliminary study, di-unsaturated acyl chains were used for the phospholipids in the leakage studies to avoid effects from phase transitions. Though the results in general cannot be directly compared with the MD simulation, this investigation can prove very useful in determining whether a lipid head group influences the degree of interaction.

To assess the effect of liposome-lipid charge on ceragenin CSA-13 activity, we also measured leakage from mixed lipid vesicles consisting of DOPG:DOPE at a molar ratio of 7:3 and 3:7. Due to the fact that liposomes composed of pure DOPE lipid are not stable enough at a neutral pH and room temperature, we considered a system with pure DOPC lipids as representative of mammalian cells.

The effects of lipid composition on calcein release induced by ceragenin CSA-13 is shown in Figure 5. We observed that CSA-13 induces significant calcein leakage of negatively charged DOPG vesicles, but exhibits weak dye-leakage activity when interacted with neutral DOPC vesicles. This finding is in accordance with the MD calculations, which suggested strong interactions between the ceragenin CSA-

13 and the negatively charged membrane. Interestingly, it is likely that in a mixed liposomal vesicle of PG and PE, ceragenin CSA-13 was very effective at inducing leakage at a higher PE content. Further investigation is needed to examine the importance of the zwitterionic lipid component on the membrane-disrupting activity of ceragenin CSA-13.
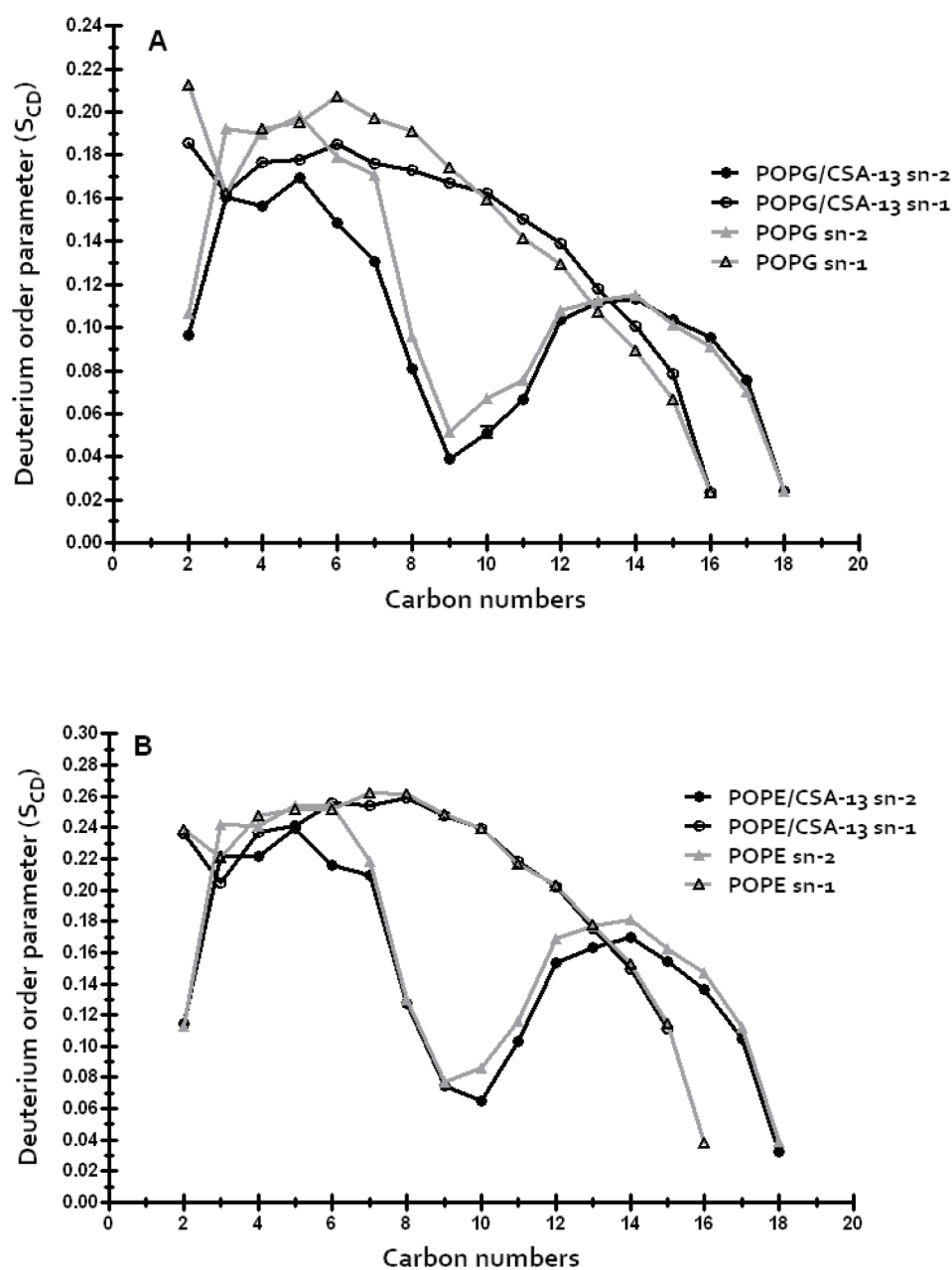

Figure 4. Order parameter profile for the lipid acyl chains of (A) POPG and (B) POPE. The deuterium order parameters are plotted for sn1 of lipids in the ceragenin CSA-13-free monolayer (open triangles), and in the monolayer in which the ceragenin CSA-13 bind (open circles); sn2 of lipids in the ceragenin CSA-13-free monolayer (solid triangles), and in the monolayer, in which the ceragenin CSA-13 bind (solid circles).
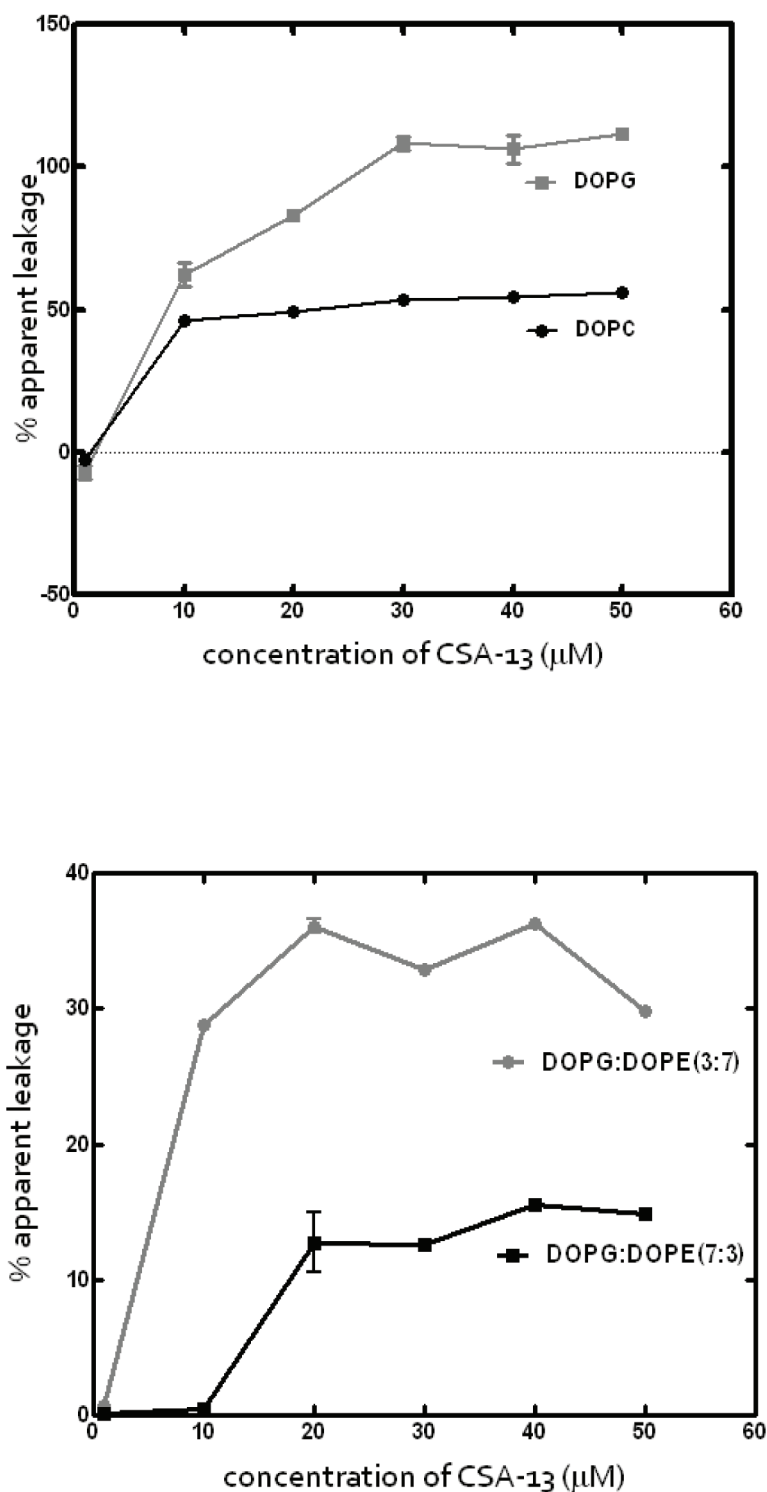
Figure 5. Leakage of calcein from phospholipid vesicles induced by ceragenin CSA-13. Each point represents the mean ± SEM of 3 experiments.

CONCLUSION

A combined experimental and simulation approach can help to better understand the interaction of ceragenin CSA-13 with lipid membranes. In summary, MD calculations demonstrated that ceragenin CSA-13 shows a clear tendency for preferential binding to the negative PG lipids (a model

membrane of bacteria) which correlate well with the leakage characteristics of liposomes. Moreover, MD simulations showed that ceragenin CSA-13 causes the destabilization of the PG-containing membrane by increasing the membrane fluidity. Our findings also indicated that ceragenin CSA-13 has an advantage in discriminating between bacterial and mammalian cells. It can, therefore, serve as a template for developing novel structures with efficacy against clinically important, multi-drug resistant pathogens. In-depth theoretical analysis of factors involved in the membrane destabilizing effect of ceragenin CSA-13, and experiments investigating such an effect on liposomes of varying lipid composition are in progress in our laboratory.

ACKNOWLEDGEMENT

REFERRENCES

1. Chin JN, Jones RN, Sader HS, Savage PB, Rybak MJ. Potential synergy activity of the novel ceragenin, CSA-13, against clinical isolates of Pseudomonas aeruginosa, including multidrug-resistant P. aeruginosa. *J Antimicrob Chemoth* 2008;61(2):365-70.

2. Aher NG, Pore VS, Mishra NN, Shukla PK, Gonnade RG. Design and synthesis of bile acid-based amino sterols as antimicrobial agents. *Bioor Med Chem Letters* 2009;19(18):5411-4.

3. Lai XZ, Feng Y, Pollard J, Chin JN, Rybak MJ, Bucki R, *et al*. Ceragenins: cholic acid-based mimics of antimicrobial peptides. *Acc Chem Res* 2008;41(10): 1233-40.

4. Giuliani A, Rinaldi A. Beyond natural antimicrobial peptides: multimeric peptides and other peptidomimetic approaches. *Cell Mol Life Sci* 2011;68(13):2255-66.

5. Epand RF, Pollard JE, Wright JO, Savage PB, Epand RM. Depolarization, Bacterial Membrane Composition, and the Antimicrobial Action of Ceragenins. *Antimicrob Agents Chemother* 2010 September 1, 2010;54(9):3708-13.

6. Epand RF, Savage PB, Epand RM. Bacterial lipid composition and the antimicrobial efficacy of cationic steroid compounds (Ceragenins). *Biochim Biophys Acta* 2007;1768(10):2500-9.

7. Brooks BR, Bruccoleri RE, Olafson BD, States DJ, Swaminathan S, Karplus M. CHARMM: A program for macromolecular energy, minimization, and dynamics calculations. *J Comp Chem*. 1983;4(2): 187-217.

8. Pastor RW, Mackerell AD, Jr. Development of the CHARMM Force Field for Lipids. *J Phys Chem Lett* 2011;2(13):1526-32.

9. Vanommeslaeghe K, Hatcher E, Acharya C, Kundu S, Zhong S, Shim J, *et al*. CHARMM general force field: A force field for drug-like molecules compatible with the CHARMM all-atom additive biological force fields. *J Comp Chem* 2010;31(4): 671-90.

10. Jorgensen W, Chandrasekhar J, Madura J, Impey R, Klein M. Comparison of simple potential functions for simulating liquid water. *J Chem Phys*. 1983;79(2): 926-35.

11. Pimthon J, Willumeit R, Lendlein A, Hofmann D. Membrane association and selectivity of the antimicrobial peptide NK-2: a molecular dynamics simulation study. *J Pept Sci* 2009;15 (10):654-67.

12. Sroda K, Michalak K, Maniewska J, Grynkiewicz G, Szeja W, Zawisza J, *et al*. Genistein derivatives decrease liposome membrane integrity--calcein release and molecular modeling study. *Biophys Chem* 2008;138(3):78-82.